Friction and Wear Properties of Basalt Fiber Reinforced/ Solid Lubricants Filled Polyimide Composites Under Different Sliding Conditions

Xinrui Zhang,[1,2] Xianqiang Pei,[1] Qihua Wang[1]

[1]*State Key Laboratory of Solid Lubrication, Lanzhou Institute of Chemical Physics, Chinese Academy of Sciences, Lanzhou 730000, China*
[2]*Graduate School, Chinese Academy of Sciences, Beijing 100039, China*

Received 8 December 2008; accepted 25 March 2009
DOI 10.1002/app.30517
Published online 24 June 2009 in Wiley InterScience (www.interscience.wiley.com).

ABSTRACT: Short basalt fibers (BFs)-reinforced polyimide (PI) composites filled with MoS_2 and graphite were fabricated by means of hot-press molding technique. The tribological properties of the resulting composites sliding against GCr15 steel ring were investigated on a model ring-on-block test rig. The wear mechanisms were also comparatively discussed, based on scanning electron microscopic examination of the worn surface of the PI composites and the transfer film formed on the counterpart. Experimental results revealed that MoS_2 and graphite as fillers significantly improved the wear resistance of the BFs-reinforced polyimide (BFs/PI) composites. For the best combination of friction coefficient and wear rate, the optimal volume content of MoS_2 and graphite in the composites appears to be 40 and 35%, respectively. It was also found that the tribological properties of the filled BFs/PI composites were closely related with the sliding conditions such as sliding speed and applied load. Research results show that the BF/PI composites exhibited better tribological properties under higher PV product. © 2009 Wiley Periodicals, Inc. J Appl Polym Sci 114: 1746–1752, 2009

Key words: basalt fiber; polymeric composites; solid lubricants; friction and wear

INTRODUCTION

Short fiber reinforced polymers composites find their applications in various fields of engineering and form a very important class of tribo-materials.[1–6] Despite lower mechanical properties in comparison with continuous fiber reinforced polymers, short fiber reinforced polymers are very attractive due to their advantages of easy fabrication.[2,4] Many investigations have shown that incorporation of fiber improved the wear resistance and reduced the friction coefficient.[1–6] Typical wear mechanisms of polymer matrix composites are fiber breaking, fiber–matrix debonding, and matrix fracture. Other important mechanisms are fiber pullout, matrix wear related to fiber movement, pealing-off of the matrix, shear deformation of the fibers, and deformation of the edges of the wear track.[7–12] Generally, the transfer film formed during the initial sliding period has the most significant effect on the friction and wear properties. The tribological properties of fiber-reinforced polymer composites can be altered by adding solid lubricants, allowing for easy shear and sometimes better thermal conductivity of polymer composites. Internal lubricants such as polytetrafluoroethylene (PTFE) and graphite flakes are frequently incorporated to improve the wear resistance and reduce the friction coefficient.[13,14] Moreover, solid lubricants should be added in narrowly defined percentages to find an optimum of tribological properties. Apart from the composition, the friction and wear behavior of the polymer composites depends on the sliding conditions.[15–19] Dickens and Sullivan[19] found that the steady state wear rate of polyphenylene oxide (PPO), polyetheretherketone (PEEK), and PTFE increased with increasing sliding speed, and that the friction coefficient of PPO and PEEK was not greatly affected, whereas the friction coefficient increased in the case of PTFE.

Polyamides (PI) attract extensive concern from tribological scientists worldwide because of their high mechanical strength, acceptable wear resistance under certain conditions, good thermal stability, high-stability under vacuum, good anti-radiation, and good solvent resistance. They are mainly used in combination with additives and fiber reinforcement for good sliding properties.[20] Basalt fibers have several advantages such as the absence of a

Correspondence to: Q. Wang (wangqh@lzb.ac.cn).
Contract grant sponsor: National Natural Science Foundation of China; contract grant number: 50805139.
Contract grant sponsor: Chinese Academy of Sciences; contract grant number: KGCX3-SYW-205.

carcinogenic effect, environmental cleanness, flexibility, good temperature resistance and heating insulation property, etc. in comparison with glass and asbestos fibers.[21] The investigations of basalt fibers (BFs)-reinforced polymer composites have been actively pursued. Currently, most studies focused on the processes and mechanical and physical properties of basalt fibers. Few works dealt with the tribological properties of BFs-reinforced polymer composites systematically. Our previous studies showed that addition of BFs can improve the tribological properties of PI composites, and BFs/PI composites exhibited better tribological properties under higher load and sliding speed.[22] The development of fiber-reinforced and solid lubricants filled polymer composites for use in actual service requires good understanding of the friction and wear mechanism.

In this experiment, BFs-reinforced PI composites filled with MoS_2 and graphite were fabricated. The purpose of this study is to investigate the effects of the two solid lubricants, sliding time, sliding speed, and applied load on the tribological properties of the BFs/PI composites. It is expected that this work will broaden the application of basalt fibers reinforced polymer composites.

EXPERIMENTAL

Samples preparation

PI (YS-20) powders (<75 μm) were commercially obtained from Shanghai Synthetic Resin Institute (Shanghai, China). The chemical structure of PI is shown in Figure 1. MoS_2 powder (<1.5 μm) and graphite powder (<1.5 μm) were provided by Shanghai Colloid Chemical Plant (Shanghai, China). The short BFs (3–4 mm), supplied by Sichuan Aerospace Tuoxin Basalt Co., Ltd., Chendu, China, were about 13 μm in diameter, the density of which was about 2.65 g/cm^3. The commercial short BFs were dipped in acetone for 24 h and then cleaned ultrasonically with clean acetone for 0.5 h. Finally, they were dried before used. The BFs/PI composites were fabricated by means of hot-press molding technique. The volume contents of the graphite (10, 20, 30, 35, 40%) and MoS_2 (10, 20, 30, 40, 50%) were chosen to study the effects of filler content on the improvement of tribological behavior. The mixtures were compressed and heated to 380°C in a mold with intermittent deflation. The pressure was held at 40 MPa for 70 min to allow full compression sintering. At the end of each run of compression sintering, the resulting specimens were cooled in the stove in air and cut into preset sizes for friction and wear tests.

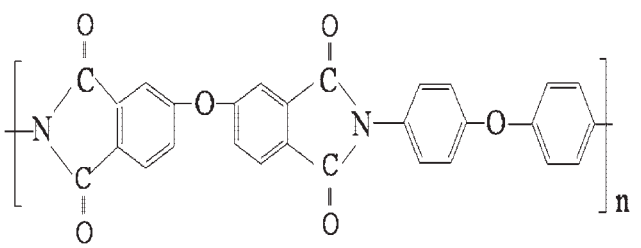

Figure 1 The chemical structure of PI powder.

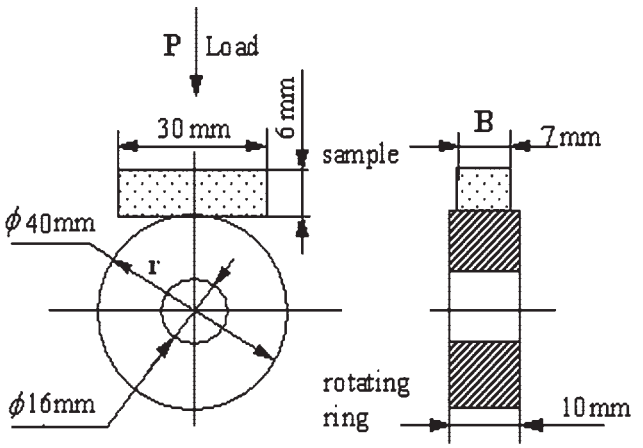

Figure 2 The contact schematic for the friction couple.

Friction and wear tests

The friction and wear behavior of the BFs/PI composites sliding against stainless steel rings were evaluated on an M-2000 model ring-on-block test rig (made by Jinan Testing Machine Factory, China). The contact technical drawing is shown in Figure 2; the chemical composition of GCr15 steel ring is shown in Table I. The tests were carried out at a linear velocity of 0.431/0.862 m/s in a period of 120 min with the loads ranging from 200 to 500 N. Before each test, the GCr15 steel ring and the composite block were polished to a roughness (Ra) of about 0.2 μm. The block specimen was static and the steel ring slid against the block unidirectionally in the friction process. The friction force was measured by using a torque shaft equipped with strain gauges mounted on a vertical arm that carried the block, which was used to calculate the friction coefficient by taking into account the applied load. The width of the wear tracks was measured with a reading microscope to an accuracy of 0.01 mm. The width of the wear tracks was measured with a reading microscope to an accuracy of 0.01 mm. Then the specific wear rate [ω, mm^3/(N m)] of the specimen was calculated as follows[23]:

TABLE I
Chemical Composition of the GCr15 Steel Ring

Chemical composition (mass fraction, %)					
C	Mn	Si	P	S	Cr
0.95–1.05	0.25–0.45	0.15–0.35	≤0.025	≤0.025	1.40–1.65

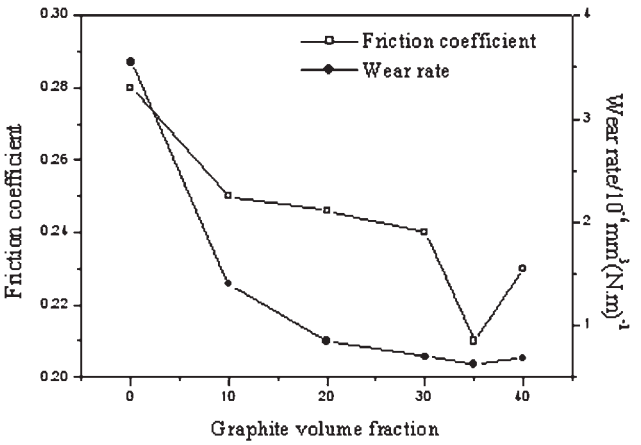

Figure 3 Variations of the friction coefficient and wear rate with various graphite contents in the BFs/PI composites.

$$\omega = \frac{B}{L \times P}\left[\frac{\pi r^2}{180}\arcsin\left(\frac{b}{2r}\right) - \frac{b}{2r}\sqrt{r^2 - \frac{b^2}{2}}\right]$$

where B is the width of the specimen (mm), r is the semi diameter of the stainless steel ring (mm), b is the width of the wear trace (mm), L is the sliding distance in meter, and P is the load in Newton. In this study, three replicated wear results were averaged and taken as the wear results.

Worn surface analysis

The morphologies of the worn surfaces of BFs/PI composites and the transfer film formed on the counterpart steel rings were analyzed on a JSM-5600LV scanning electron microscope (SEM). To increase the resolution for the SEM observation, the tested specimens were plated with gold coating to render them electrically conductive.

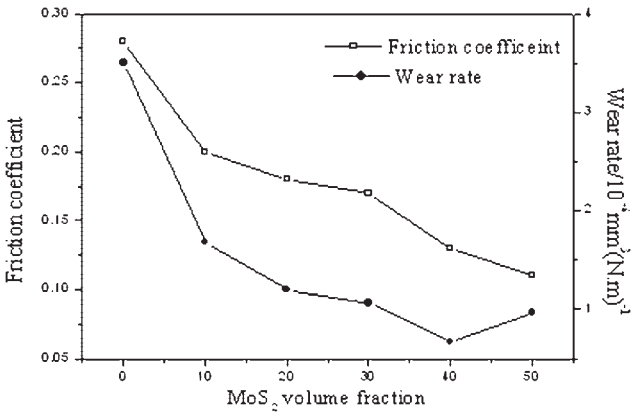

Figure 4 Variations of the friction coefficient and wear rate with various MoS_2 contents in the BFs/PI composites.

RESULTS AND DISCUSSION

Volume fraction of solid lubricants

The friction coefficient and wear rate of BFs/PI composites with various graphite contents at 0.431 m/s and 200 N are shown in Figure 3. It can be found that graphite was effective in improving the friction and wear behavior of BFs/PI composites, especially the anti-wearability of the composites. There is a significant reduction in the friction coefficient and wear rate with 10% graphite. With an increase in the content, the declining trend becomes gentle. In the tested system, the optimal volume content of graphite was about 35%. Further addition of graphite increases the friction coefficient and wear rate, which means excessive graphite tend to conglomerate and lead to less uniformity of the system and thus reduce the anti-wearability of the composites. In Figure 4, the friction coefficient and wear rate of MoS_2-filled BFs/PI composites are plotted versus the volume contents of MoS_2. With the addition of MoS_2, both the friction coefficient and the wear rate reduced. The wear rate decreased with increasing

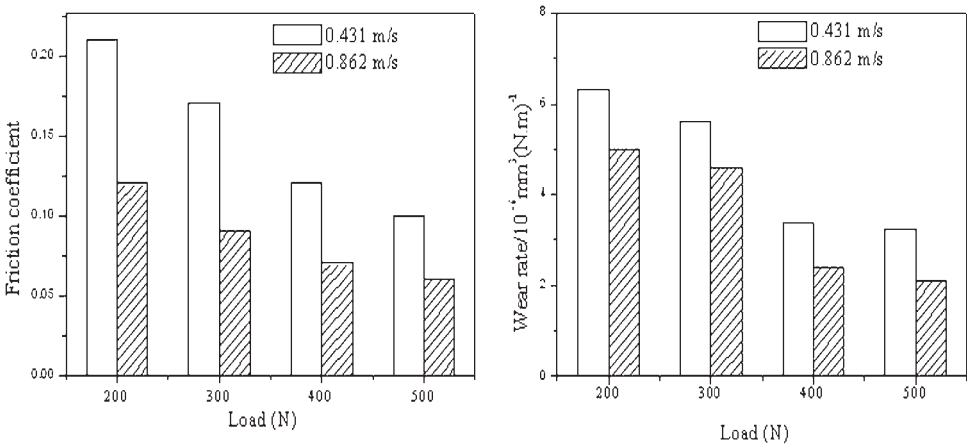

Figure 5 Effects of load and sliding speed on coefficient of friction of the BFs/PI composites filled with graphite.

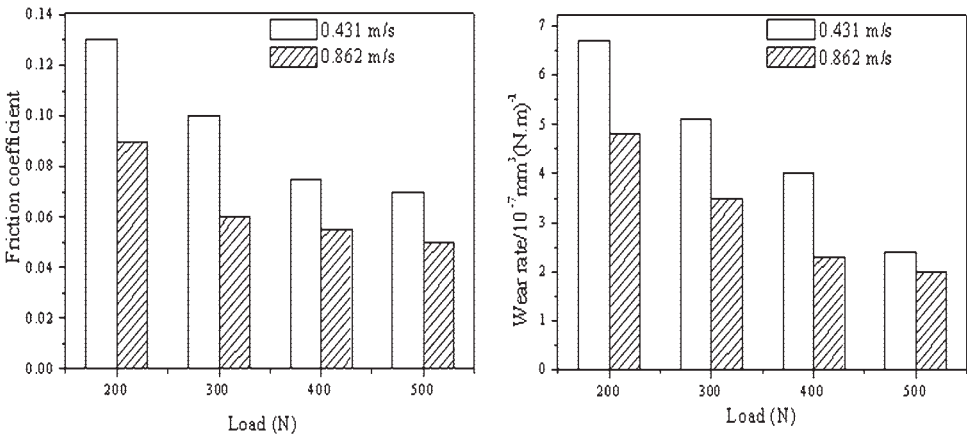

Figure 6 Effects of load and sliding speed on coefficient of friction of the BFs/PI composites filled with MoS_2.

MoS_2 volume content up to 40%, and then increased, while the friction coefficient decreased with increasing MoS_2 content. For the best combination of friction coefficient and wear rate, the optimal volume content is 40% according to the friction-reduction and anti-wearabilities. 40% MoS_2 and 35% graphite-filled BFs/PI composites were chosen to investigate the effects of the applied load and sliding speed on the friction and wear behavior of the BFs/PI composites.

The friction coefficient and wear rate as a function of load and sliding speed for the BFs/PI composites filled with graphite and MoS_2 powders are depicted in Figures 5 and 6, respectively. Evidently, regardless of sliding speed, the friction coefficient of the composites decreased with increasing load. Similar results have been reported by various researchers for PTFE composites.[24] A common explanation is the equation $\mu = kN^{n-1}$ (where μ is the friction coefficient, N is the load, and k and n are constants with n between 2/3 and 1, depending on the amount of interaction between elastic and plastic deformation).[24,25] It is also clearly seen that the friction coefficient decreased obviously under high sliding speed compared with that under low sliding speed with an increase in load. Moreover, the influence of sliding speed on the friction coefficient became less significant under higher load. With an increase in sliding speed, there was not enough time to produce more adhesive points owing to the decreased surface contact time. As a result, the friction force component from adhesion can be greatly reduced and the transfer film can easily be formed and difficult to be ruptured. It is assumed that, under a small load, the interfacial temperature is a crucial factor determining the tribological characteristics.[26] Some processes with their molecular mechanism are related to the transformation of mechanical energy into heat in the friction process.[17] The increase in sliding speed will result in a higher contact temperature. Because of the low thermal conductivity of PI, friction-induced heat surely provokes an increase in the temperature of the actual contact. The friction coefficient decreased remarkably owing to the effect of thermal softening. The wear rate decreased with the increase in applied load and sliding speed. When applied load increased, the transfer film can easily be formed

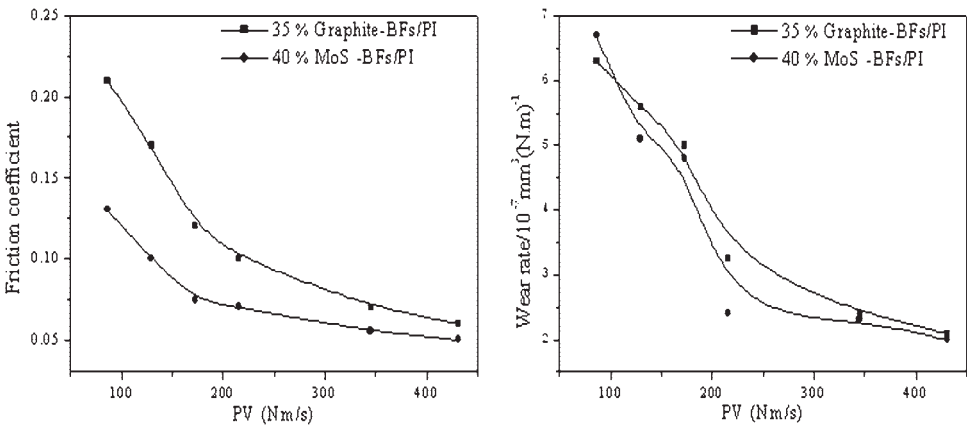

Figure 7 Friction coefficient and wear rate versus PV product.

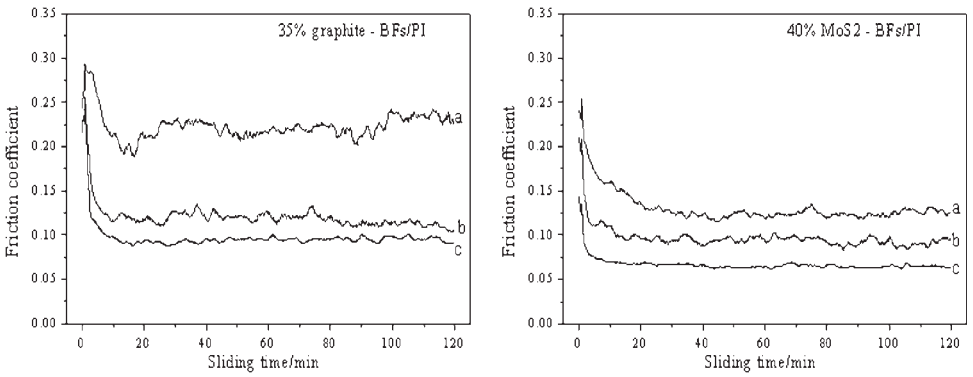

Figure 8 Effect of sliding time on the friction coefficient of the BFs/PI composites: (a) at 200 N and 0.431 m/s; (b) at 200 N and 0.862 m/s; (c) at 500 N and 0.431 m/s.

owing to the increase in adhesive force between the film and counterpart. Moreover, the newly formed debris would come into being a more integrated but thinner layer on the worn surface, which resulted in a smaller wear rate because of decreased degree of two-body abrasive wear.[27] The influence of sliding speed on the wear rate also became less significant under higher load. Clearly, the BFs/PI composites filled with MoS_2 or graphite have better tribological properties under the same PV value but a higher load and a lower sliding speed. To better understand the mechanisms involved, the friction and wear rate are re-plotted against the product of applied load and sliding speed (PV) in Figure 7. Interestingly, the friction coefficient and wear rate of the BFs/PI composites were found to be inversely proportional to the PV product. The higher the PV values, the lower the friction coefficient and wear rate. This agreed well with the result reported by Voss and Friedrich for short glass-fiber–PTFE composites.[28] Under higher PV values, solid lubricant debris get entrapped in contact region. The wear debris then form a "third body interface" and the wear mechanism changed from solid body friction to dry lubricated friction.

Figure 8 presented the typical evolutions of the friction coefficient of BFs/PI composites as a function of the sliding time under different load and sliding speed. It can be found that the friction process can be divided into two distinct stages: the one

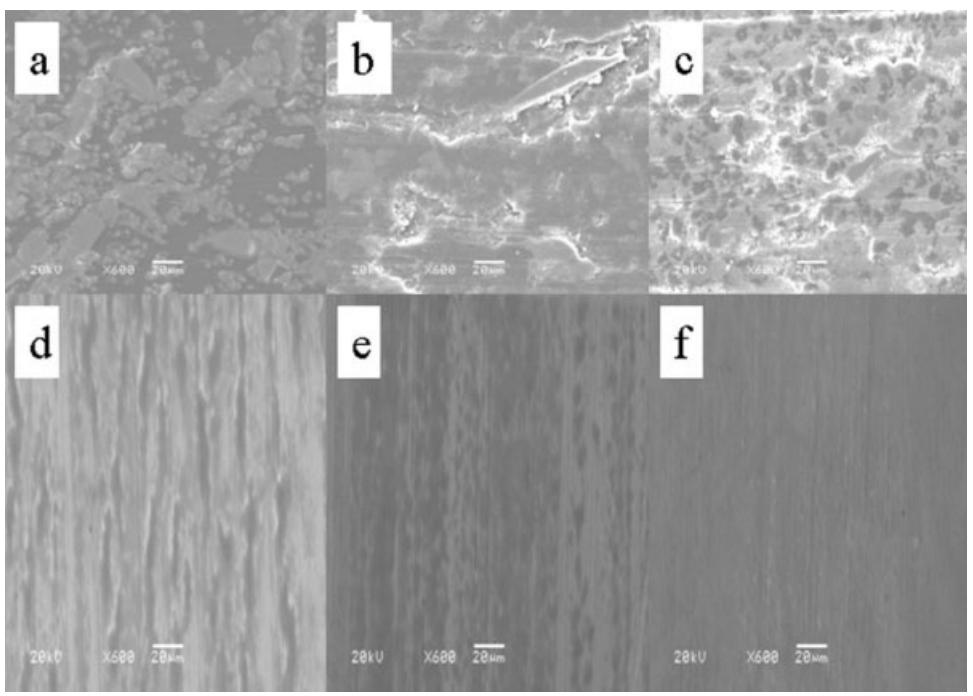

Figure 9 SEM morphologies of the worn surface and the transfer films of the BFs/PI composites: (a) Pure BFs/PI; (b) 35% graphite–BFs/PI; (c) 40% MoS_2^- BFs/PI; (d) transfer film of (a); (e) transfer film of (b); (f) transfer film of (c).

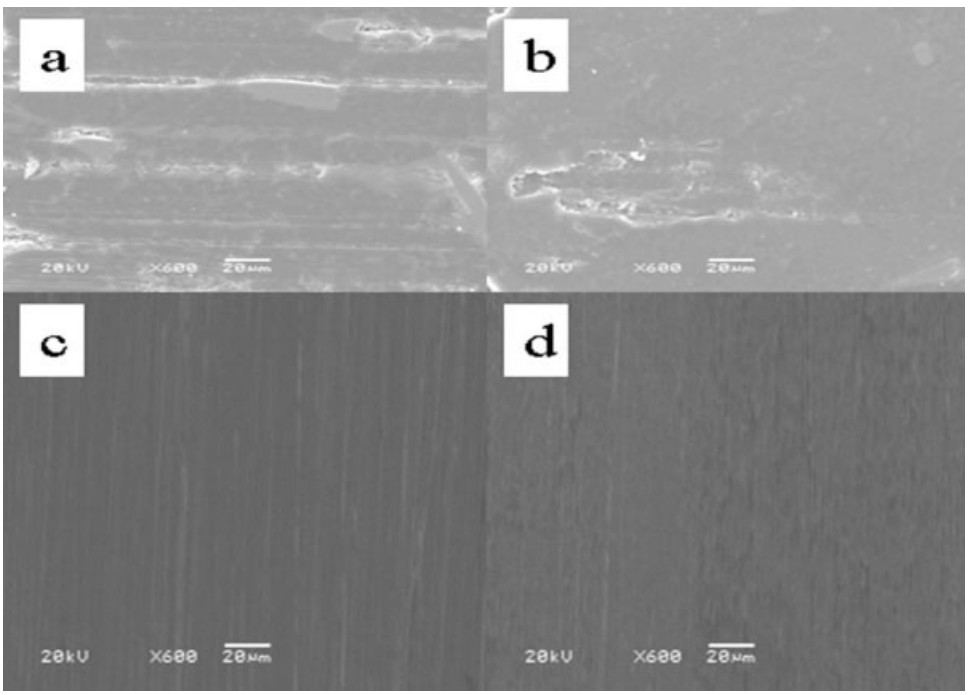

Figure 10 SEM morphologies of the worn surfaces and the transfer films of 35% graphite–BFs/PI composites sliding under different conditions: (a) 200 N, 0.862 m/s; (b) 500 N, 0.431 m/s; (c) transfer film of (a); (d) transfer film of (b).

is the running-in period and the other is the steady-state period. After the formation and the peeling-off of the transfer film came to a balance, the friction coefficient became stable. The obtained friction coefficient at the running-in period is much higher than that at the steady-state period. Moreover, the time of running-in period and friction coefficient show an obvious decrease with the increasing PV values, which are in full agreement with the results presented above.

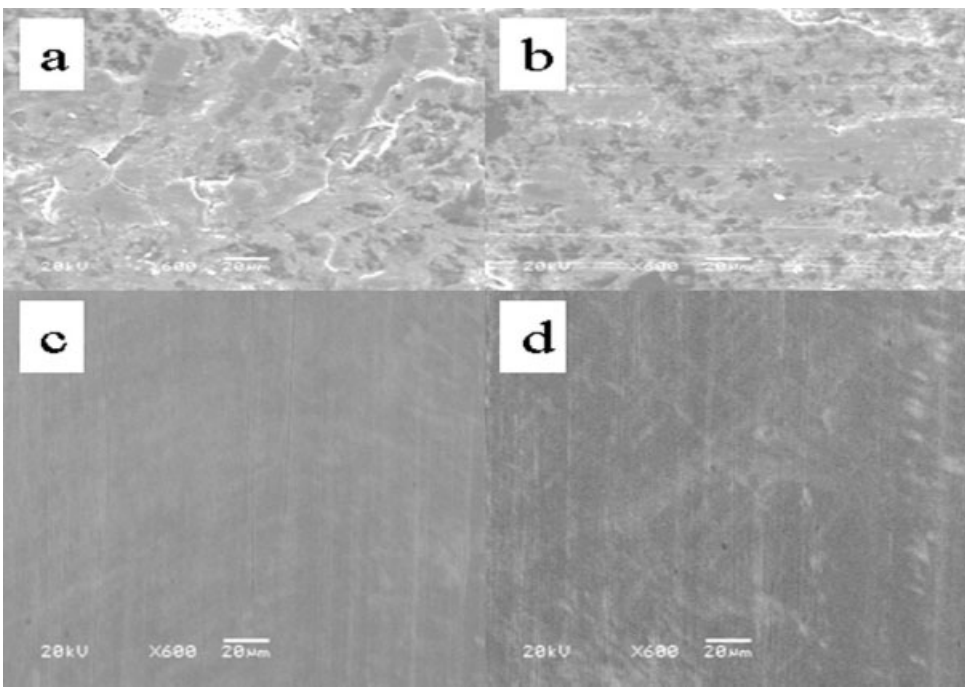

Figure 11 SEM morphologies of the worn surfaces and the transfer films of 40% MoS_2^- BFs/PI composites sliding under different conditions: (a) 200 N, 0.862 m/s; (b) 500 N, 0.431 m/s; (c) transfer film of (a); (d) transfer film of (b).

SEM analysis of worn surface and counterpart surface

Figure 9 shows SEM analysis of the worn surfaces and the transfer films of BFs/PI composites sliding against the GCr15 steel at 0.431 m/s and 200 N. The worn surface of the unfilled BFs/PI composites was characterized by severe abrasive wear; there existed lots of PI debris and exposure of BFs on the worn surface [Fig. 9(a)], and the transfer film [Fig. 9(d)] was thick and discontinuous, which correspond to its bad tribological properties. As for 35% graphite-filled BFs/PI composite, the worn surface [Fig. 9(b)] was characterized by adhesion wear. Meanwhile, the transfer film [Fig. 9(e)] became thinner but still not uniform. The worn surface of 40% MoS_2-filled BFs/PI composite [Fig. 9(c)] was characterized by adhesion wear and fatigue wear. There were no obvious scuffing phenomena on the worn surface. The transfer film [Fig. 9(f)] became comparatively thinner and more coherent.

As for 35% graphite-filled BFs/PI composite, the worn surface [Fig. 10(a)] became smoother and there appeared more integrated wear debris oriented along the sliding direction under high sliding speed; the transfer film became thinner and more uniform [Fig. 10(c)]. It can be seen that there existed a more integrated layer on the worn surface [Fig. 10(b)] under higher applied load. When the applied load increased, some big particle-shaped or flaky debris in the wear surface would be crushed or sheared into smaller particles or thinner flakes and acted as lubricants; the newly formed debris would come into being a more integrated layer on the worn surface and reduced the "direct contact" between the BFs/PI composite and the counterpart, which agrees well with the improved tribological properties of the BFs/PI composites.[25] The transfer film [Fig. 10(d)] becomes progressively homogeneous and enhances self-lubricating properties of the BFs/PI composites. As for 40% MoS_2-filled BFs/PI composites, the worn surface [Fig. 11(a)] was characterized by slight fatigue wear, and there appeared flaky debris on the worn surface and acted as lubricants. The transfer film became more coherent and uniform [Fig. 11(c)]. The worn surface [Fig. 11(b)] was characterized by slight adhesion and fatigue wear, It can also be seen that a more integrated film existed on the worn surface. The transfer film was thin, coherent, and uniform [Fig. 11(d)]. With the formation of a more uniform and coherent transfer film, subsequent sliding occurred between the surface of the BFs/PI composites and the transfer film. Consequently, a lower friction coefficient and wear rate was reached.

CONCLUSIONS

Addition of MoS_2 and graphite can improve the tribological properties of BFs/PI composites greatly. For the best combination of friction coefficient and wear rate, the optimal volume content of MoS_2 and graphite in the BFs/PI composites appears to be 40 and 35%, respectively. The differences in the friction and wear properties of BFs/PI composites are closely related with the sliding conditions such as sliding speed and applied load. Research results show that BFs/PI composites exhibited better tribological properties under higher PV product.

References

1. Yoo, J. H.; Eiss, N. S. Wear 1993, 162, 418.
2. Bijwe, J.; Indumathi, J.; Rajesh, J. J.; Fahim, M. Wear 2001, 249, 715.
3. Xian, G.; Zhang, Z. Wear 2005, 258, 776.
4. Palabiyik, M.; Bahadur, S. Wear 2002, 253, 369.
5. Friedrich, K.; Lu, Z.; Hager, A. M. Wear 1995, 190, 139.
6. Bahadur, S.; Fu, Q.; Dong, D. Wear 1994, 178, 123.
7. Ramesh, R.; Rao, R. M. V. G. K. Wear 1983, 89, 131.
8. Chand, N.; Naik, A.; Neogi, S. Wear 2002, 242, 38.
9. El-Tayeb, N. S. M.; Mostafa, I. M. Wear 1996, 195, 186.
10. El-Tayeb, N. S. M.; Gadelrab, R. M. Wear 1996, 192, 112.
11. Pihtili, H.; Tosun, N. Compos Sci Technol 2002, 62, 367.
12. El-Sayed, A. A.; El-Sherbiny, M. G.; Abo-El-Ezz, A. S. Wear 1995, 184, 45.
13. Tanaka, K. Effects of Various Fillers on the Friction and Wear of PTFE-Based Composites; Elsevier: Amsterdam, 1986.
14. Cenna, A. A.; Dastoor, P.; Beehag, A.; Page, N. W. J Mater Sci 2001, 36, 891.
15. Lu, Z. P.; Friedrich, K. Wear 1995, 181, 624.
16. Bassani, R.; Levita, G.; Meozzi, M.; Palla, G. Wear 2001, 247, 125.
17. Myshkin, N. K.; Petrokovets, M. I.; Kovalev, A. V. Tribol Int 2005, 38, 910.
18. Flom, D. G.; Porile, N. T. Nature 1995, 175, 682.
19. Dickens, D. M.; Sullivan, J. L. Wear 1986, 112, 273.
20. Fusaro, R. L. Tribol Trans 1987, 31, 174.
21. Kuryaeva, R. G.; Kirkinskii, V. A. Phys Chem Miner 1997, 25, 48.
22. Zhang, X. R.; Xian, Q. P.; Wang, Q. H. J Appl Polym Sci 2009, 111, 2980.
23. Cai, H.; Yan, F. Y.; Xue, Q. J.; Liu, W. M. Polym Test 2003, 22, 875.
24. Unal, H.; Mimaroglu, A.; Kadioglu, U. Mater Des 2004, 25, 239.
25. Stuart, B. H. Polym Test 1997, 16, 49.
26. Zhang, G.; Zhang, C.; Nardin, P. Tribol Int 2008, 41, 79.
27. Friedrich, K.; Flock, J.; Varadi, K.; Neder, Z. Wear 2001, 251, 1202.
28. Voss, H.; Friedrich, K. J Mater Sci Lett 1986, 5, 1111.